Supporting Information

Amino-Type Halogen-Bonded Organic Framework for Selective Adsorption of Aliphatic Acid Vapors: Insight into the Competitive Interactions of Halogen Bonds and Hydrogen Bonds

Guanfei Gong[a], Jiahao Zhao[a], Yi Chen[a], Fei Xie[b], Feihong Lu[a], Jike Wang[a], Lu Wang[a], Shigui Chen*

[a]The Institute for Advanced Studies, Wuhan University, 299 Bayi Road, Wuhan, Hubei 430072, China

[b]National Synchrotron Radiation Laboratory, University of Science and Technology of China, Hefei, Anhui 230029, China

Contents

Materials and Instruments

$AgBF_4$, I_2 and triphenylamine were obtained from Bide Pharmatech Ltd and used without further purification. Other starting materials were obtained from commercial suppliers and used without further purification. Analytical thin-layer chromatography (TLC) was performed on silica-gel plate w/UV254 (200μm). The ^1H NMR spectrum was recorded on 600 MHz spectrometer (BRUKER, Ascend 600) in the indicated solvents. Chemical shifts are expressed in parts per million (δ) using residual solvent protons as the internal standard. The couple constants values *(J*) are recorded in Hertz (Hz). Powder XRD patterns were recorded on Rigaku Smart Lab SE Automated Multipurpose X-ray Diffractometer. Nitrogen adsorption and desorption isotherms were recorded with a Micromeritics ASAP 2020M system at 77 K. IR spectra were recorded on Agilent Cary 630 FTIR spectrograph. X-ray photoelectron spectroscopy (XPS) was performed in ESCALAB 250Xi (The adventitious carbon located at 284.8 eV was used to calibrate samples without the carbon themselves). The morphologies of XOF were characterized using transmission electron microscopy (JEM-F200). The fluorescent photos of the solid powder were recorded using Laser Scanning Confocal Microscope (LSCM, Leica TCS SP8 MP). Fluorescence spectra were recorded on a HITACHI F-4700 spectrofluorophotometer. The SAXS experiments were carried out at the 1W2A small-angle scattering beamline of the Shanghai Synchrotron Radiation Facility.

Scheme S1. Synthesis of **TPPA** and **TPhA.**

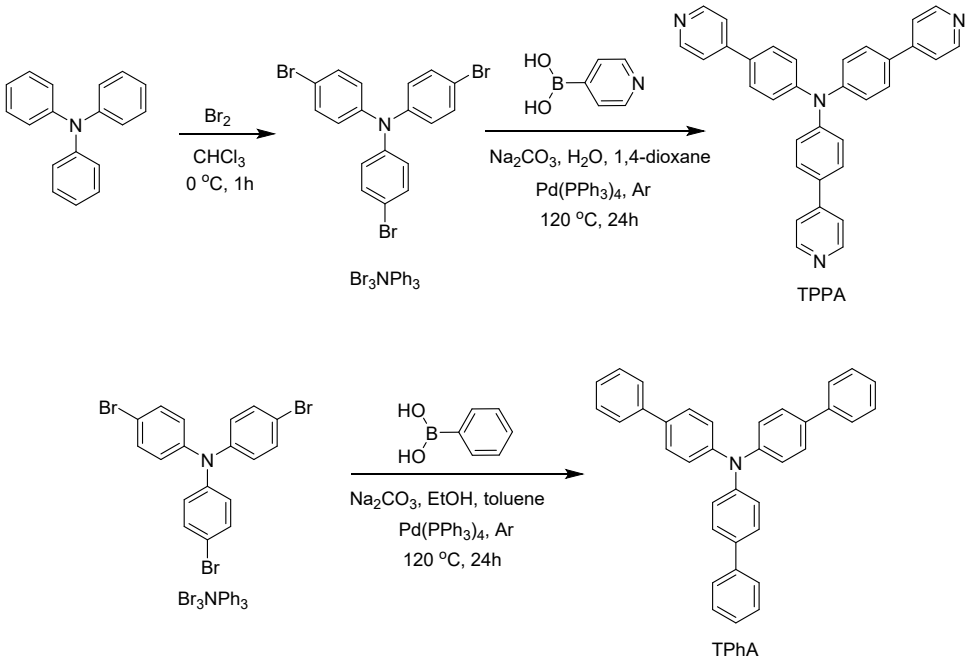

Synthesis of tris(4-bromophenyl) amine[1]:

Bromine (11.7g, 3.80 mL, 0.073 mol) dissolved in chloroform (10 mL) was injected to a solution of triphenylamine (6.00 g, 25.00 mol) in chloroform (40 mL) over a time period of 30 min at 0 °C. After stirring the solution at room temperature for additional 30 min, the solvent was evaporated in vacuo. The resulting solid was dissolved in a small amount of chloroform and 100 mL of hot ethanol was added. After the solution is cooled in an ice bath, tris(4- bromophenyl) amine crystallizes as colourless needles (Yield: 9.50 g, 81%). ^1H-NMR ($CDCl_3$, 600 MHz). δ (ppm): 6.91 (d, *J* = 6.0 Hz, 6H), 7.34 (d, *J* = 6.0 Hz, 6H).

Synthesis of tris(4-(pyridin-4-yl)phenyl)amine[2]:

A mixture of tris (4-bromophenyl) amine (3.00 g, 6.20 mmol), $Pd(PPh_3)_4$ (0.36 g, 0.31 mmol), pyridine-4-boronic

acid (4.27 g, 34.70 mmol), K_2CO_3 (6.85 g, 49.60 mmol), 1,4-dioxane (150 mL) and water (7 mL) were degassed with a steady stream of N_2 for 15 min at room temperature. The reaction mixture was then heated to reflux for 24 h in nitrogen atmosphere. After cooling to room temperature, the reaction mixture was extracted by $CHCl_3$ (3×150 mL). The combined organic layers were washed with brine, dried over $MgSO_4$, and evaporated in vacuo. The residue was purified by silica gel column chromatography with EA as eluent to give the target compound **TPPA** as yellow solid (Yield: 2.50 g, 85 %). ^{1}H NMR (DMSO-d_6, 600 MHz). δ (ppm): 8.62 (d, J = 6 Hz, 4H), 7.85 (d, J = 6.0 Hz, 6H), 7.75 (d, J = 6 Hz, 4H), 7.24 (d, J = 6.0 Hz, 6H).

Synthesis of TPhA:

A mixture of tris (4-bromophenyl) amine (0.48 g, 1.00 mmol), $Pd(PPh_3)_4$ (115 mg, 0.10 mmol), pyridine-4-boronic acid (0.61 g, 5.00 mmol), Na_2CO_3 (1.60 g, 15.20 mmol), toluene (7.5 mL) and EtOH (2.5 mL) were degassed with a steady stream of N_2 for 15 min at room temperature. The reaction mixture was then heated to reflux for 24 h in nitrogen atmosphere. After cooling to room temperature, the reaction mixture was extracted by $CHCl_3$ (3×150 mL). The combined organic layers were washed with brine, dried over $MgSO_4$, and evaporated in vacuo. The residue was purified by silica gel column chromatography with EA as eluent to give the target compound **TPhA** as white solid (Yield: 0.18 g, 25 %). ^{1}H NMR ($CDCl_3$, 600 MHz). δ (ppm): 7.60 (d, 6H), 7.53 (d, 6H), 7.44 (t, 6H), 7.33 (m, 3H) , 7.24 (d, 6H).

Preparation of MOF-TPPA and XOF-TPPA

MOF-TPPA:

$AgBF_4$ (28.5 mg, 0.15 mmol) in methanol (1 mL) was added dropwise into a solution of **TPPA** (47.6 mg, 0.1 mmol) in MeOH (3 mL) solution. The solution was degassed under freeze-pump-thaw for three cycles, and stirred for 3 h at 130 °C. Then, the solvent was removed under reduced pressure without heating. The precipitate dried under vacuum overnight.

XOF-TPPA:

$AgBF_4$ (28.5 mg, 0.15 mmol) in methanol (1 mL) was added dropwise into a solution of **TPPA** (47.6 mg, 0.1 mmol) in MeOH (3 mL) solution. After the solution was stirred for 1 hour at room temperature, iodine (37.5 mg, 0.15 mmol) in MeOH (1 mL) was added. Then, the solution was degassed under freeze-pump-thaw for three cycles, and the mixture was stirred for 3h at 130 °C. Then, the solvent was removed under reduced pressure without heating. The precipitate dried under vacuum overnight.

Adsorption–desorption experiment of XOF-TPPA to aliphatic acid vapors:

The sample of XOF-TPPA (20mg) was put in an unsealed 1.5-mL vial. The small vial was then placed in a 20-mL vial with the aliphatic acid (0.5 mL) at the bottom. The big vial was sealed at 25 °C for 24 hours to absorb the vapor completely by **XOF-TPPA**. After weighed to determine the adsorption, the sample was dried at 60 °C for 12 hours under the vacuum drying oven for the desorption. The sample was cooled to room temperature in a sealed vial.

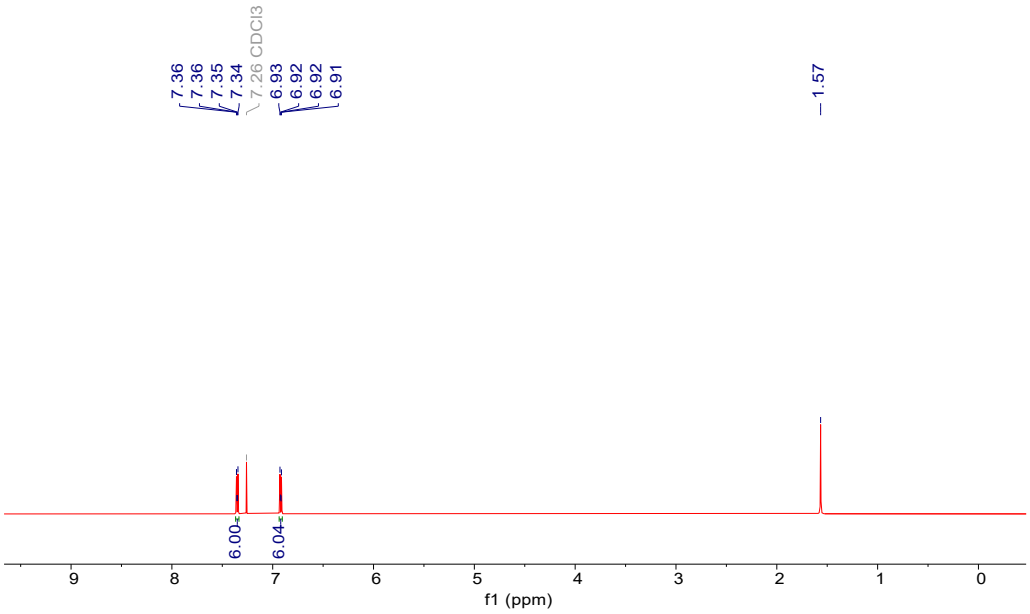

Fig. S1. ^{1}H-NMR of spectrum of **Br_3NPh_3** in $CDCl_3$ (600 MHz, 298 K)

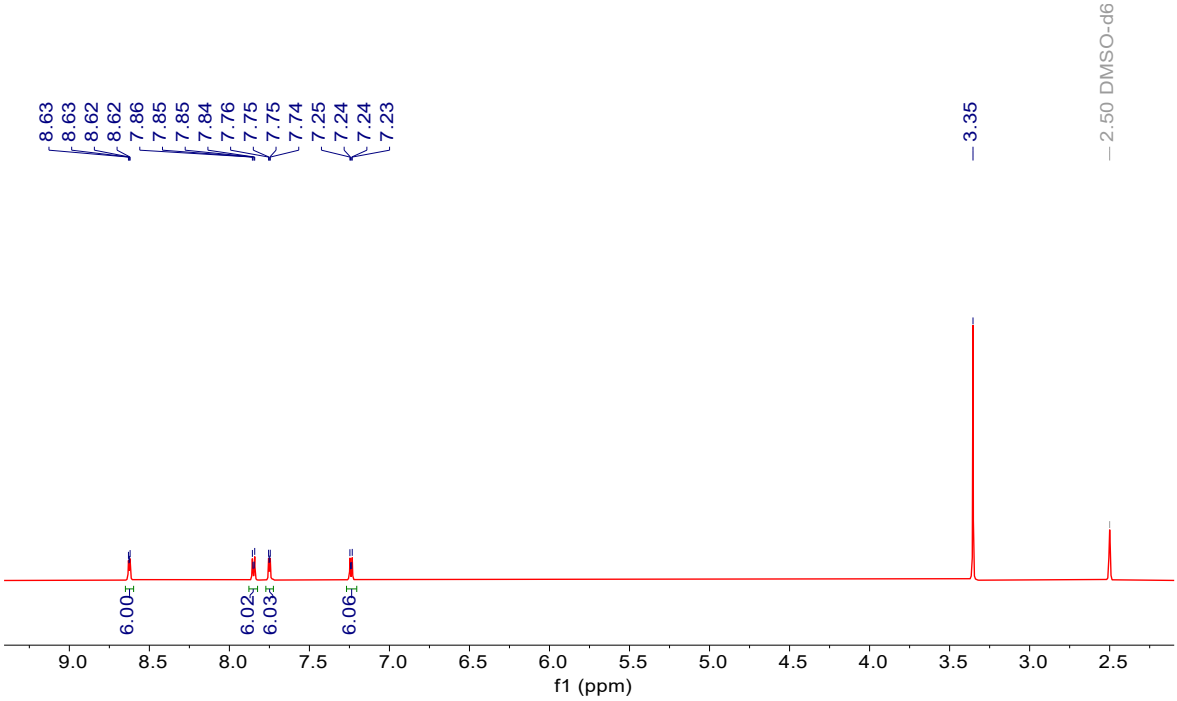

Fig. S2. ^{1}H-NMR of spectrum of **TPPA** in DMSO-d_6 (600 MHz, 298 K)

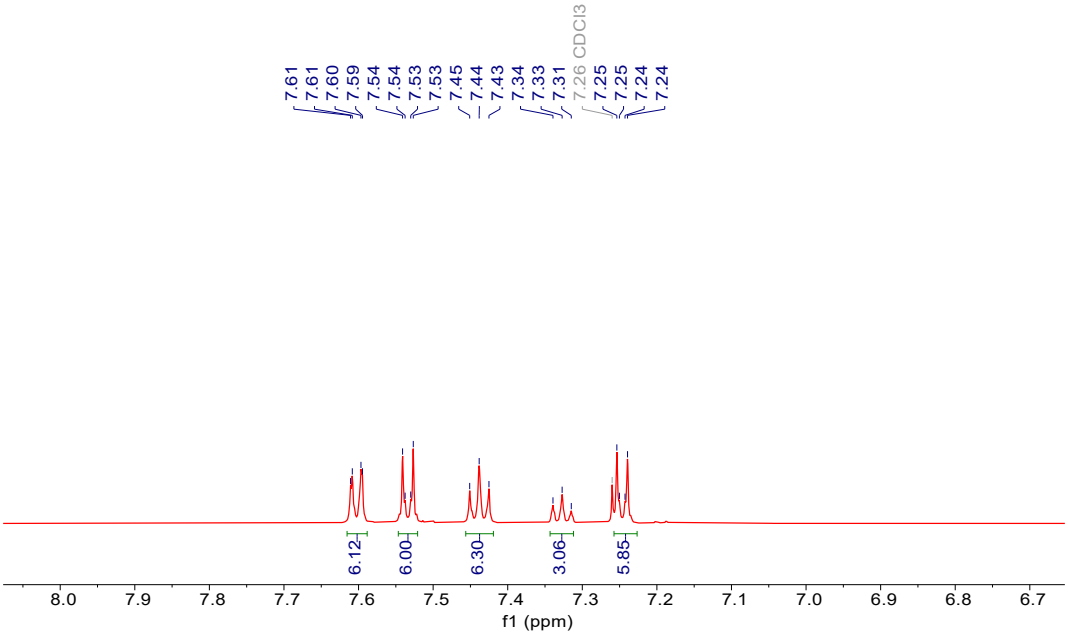

Fig. S3. ^{1}H-NMR of spectrum of **TPPA** in $CDCl_3$ (600 MHz, 298 K)

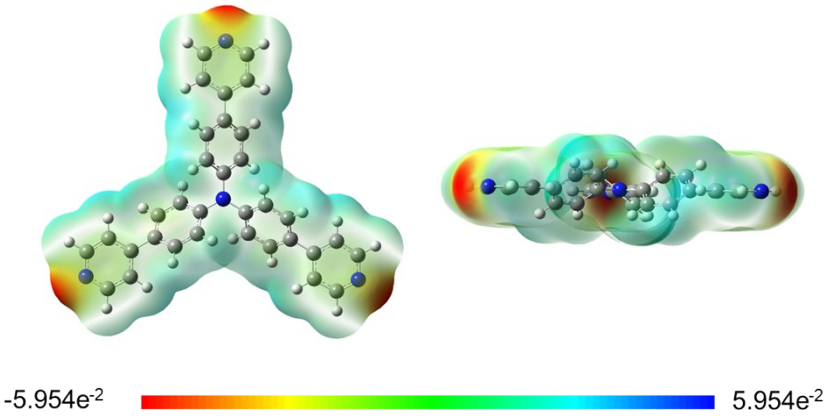

Fig. S4. Electrostatic potential ESP map of **TPPA**

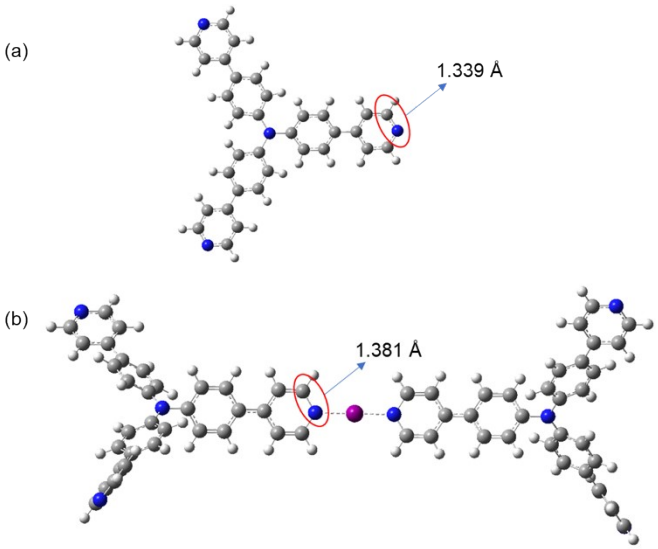

Fig. S5. Optimized geometries of **TPPA** (a) and **2TPPA@I**$^{+}$.

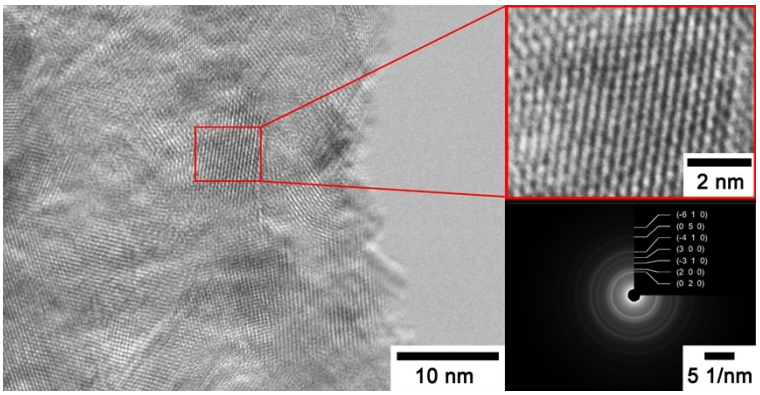

Fig. S6. TEM, HRTEM (inset) and SAED (inset) images of **MOF-TPPA**

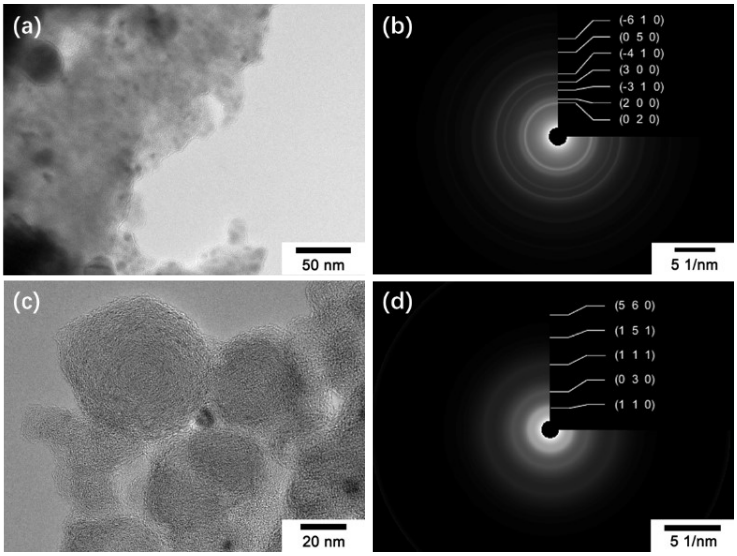

Fig.S7. Microcrystals of (a) **MOF-TPPA** as recorded by TEM and its SAED patterns (b). Microcrystals of (c) **XOF-TPPA** as recorded by TEM and its SAED patterns (d).

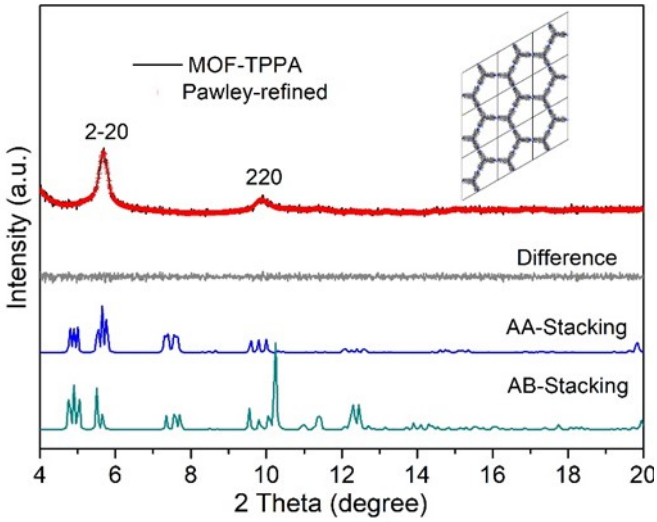

Fig. S8. Experimented (black) and refined (red) PXRD, the difference plot between the experimental and refined PXRD pattern, simulated PXRD patterns for eclipsed AA stacking and staggered AB stacking mode for **MOF-TPPA**. Inset: Top views of structural representations of **MOF-TPPA** in eclipsed AA stacking model.

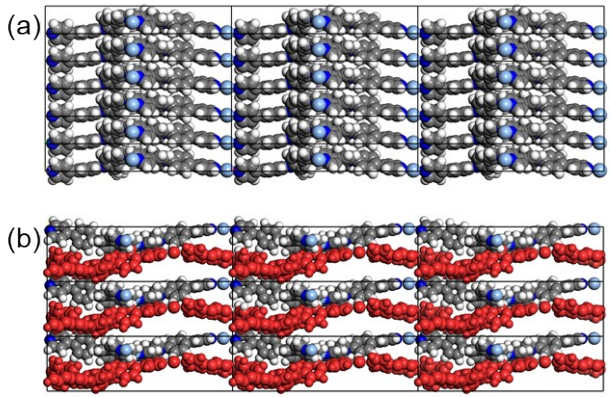

Fig. S9. (a) AA and (b) AB stacking modes of **MOF-TPPA**

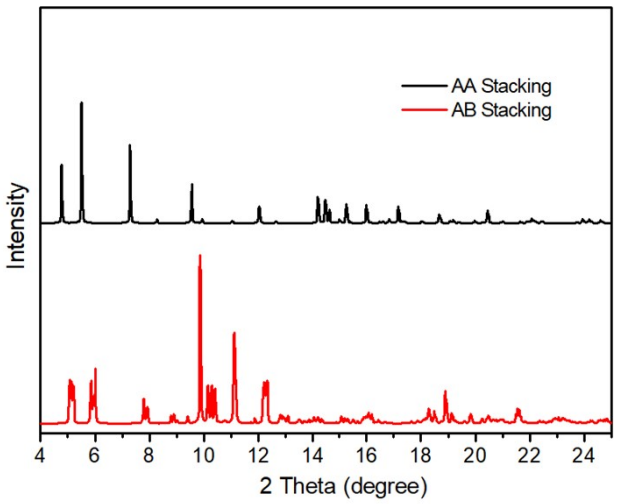

Fig. S10. Simulated PXRD patterns for eclipsed AA stacking and staggered AB stacking mode for **XOF-TPPA**.

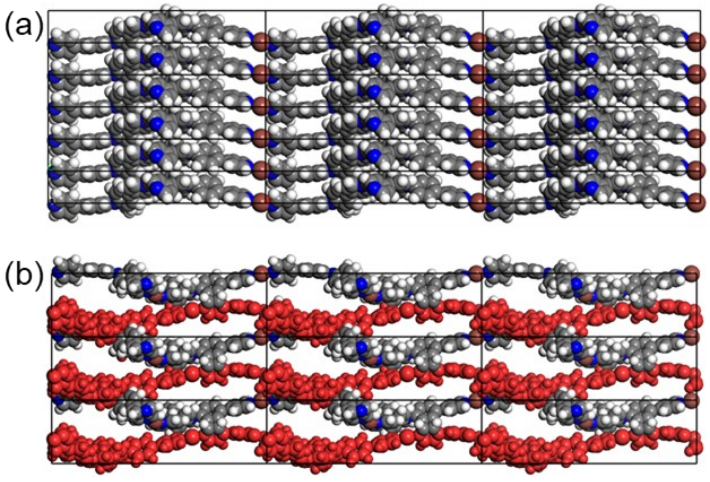

Fig. S11. (a) AA and (b) AB stacking modes of **XOF-TPPA**

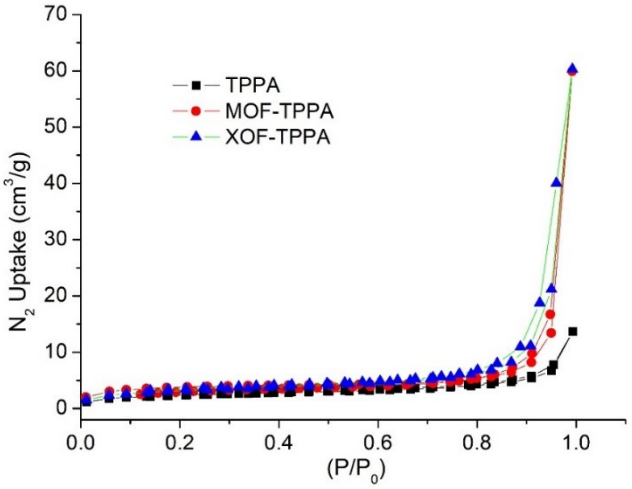

Fig. S12. N_2 adsorption isotherm at 77 K for **TPPA**, **MOF-TPPA** and **XOF-TPPA**.

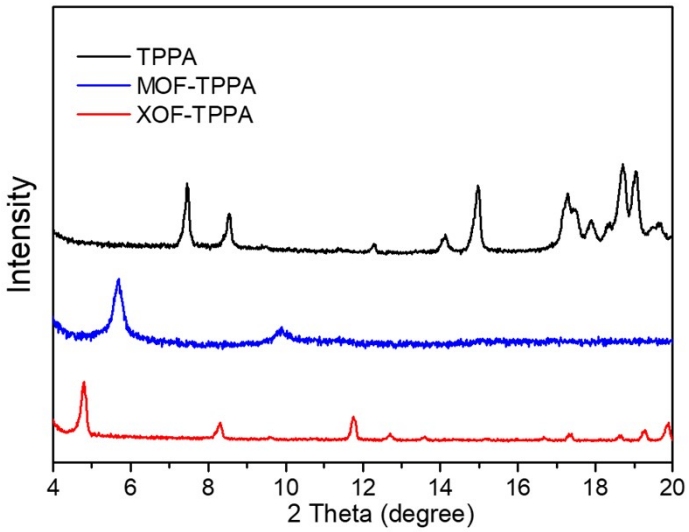

Fig. S13. Experimental PXRD patterns for **TPPA**, **MOF-TPPA** and **XOF-TPPA**.

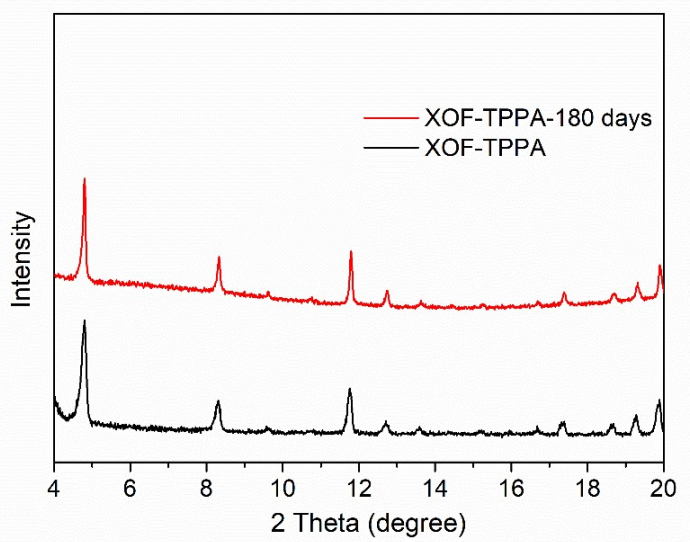

Fig. S14 The XRD patterns of **XOF-TPPA** (black), and after **XOF-TPPA** is placed at room temperature for 180 days (red)

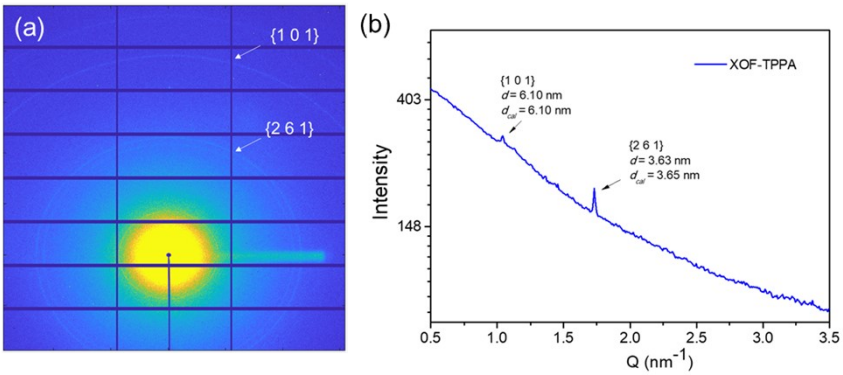

Fig. S15. (a) Solution-phase 2D SAXS image of **XOF-TPPA**; (b) Solution-phase SAXS profiles of **XOF-TPPA**

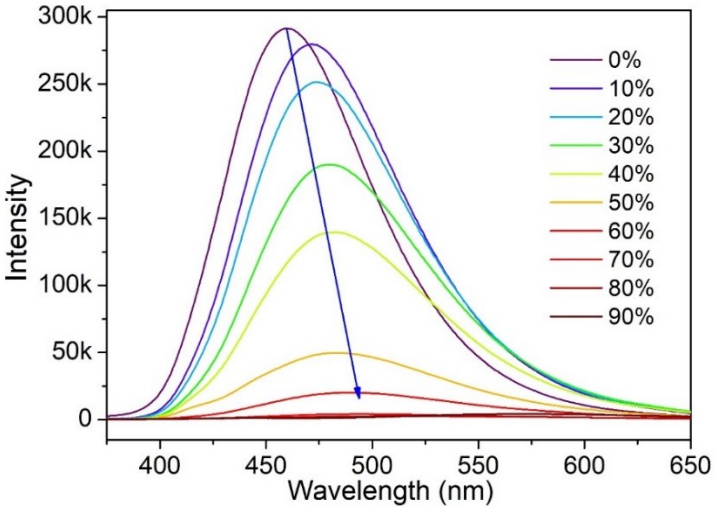

Fig. S16. Fluorescence spectrum of **TPPA** (10^{-4} M) in DMSO/H_2O mixture solution (λ_{ex} = 340 nm, Ex/Em slit = 5 nm)

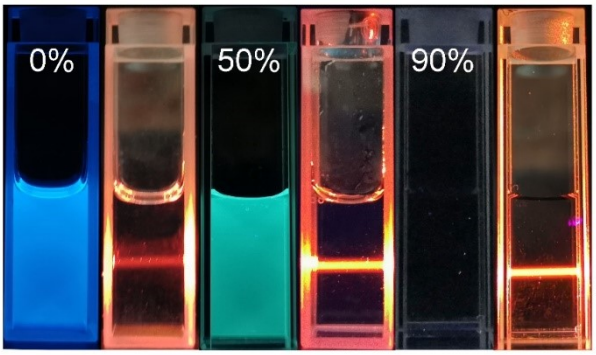

Fig. S17. Fluorescence (under a 365 nm ultraviolet lamp) and tyndall effect photos of **TPPA** in DMSO/H_2O mixtures with different water fractions

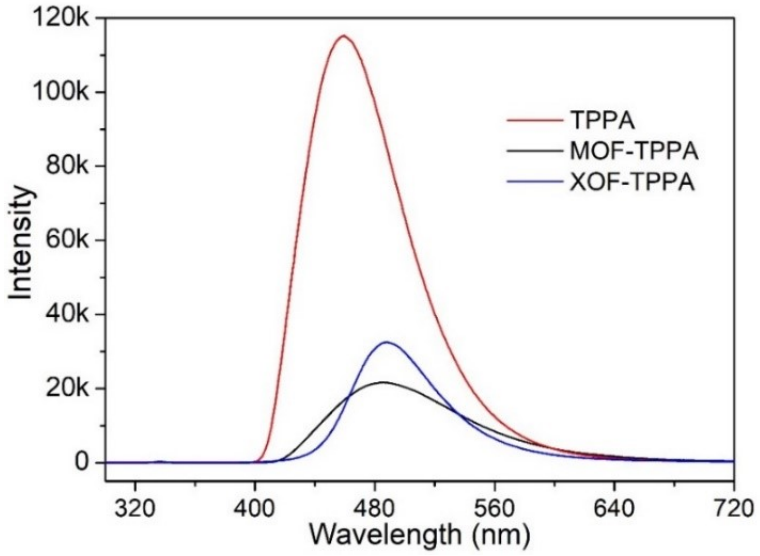

Fig. S18. Fluorescence spectra of **TPPA**, **MOF-TPPA** and **XOF-TPPA** (1 mg/ml) in DMSO solution, λex = 340 nm, Ex/Em slit = 5/5 nm

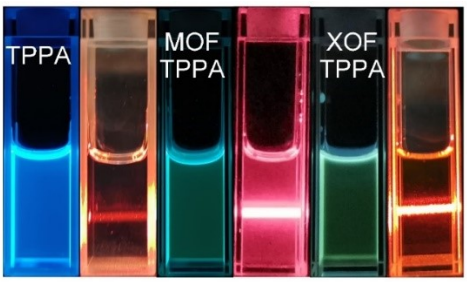

Fig. S19. Fluorescence (under a 365 nm ultraviolet lamp) and Tyndall effect photos of **TPPA**, **MOF-TPPA** and **XOF-TPPA** (1 mg/ml) in DMSO solution.

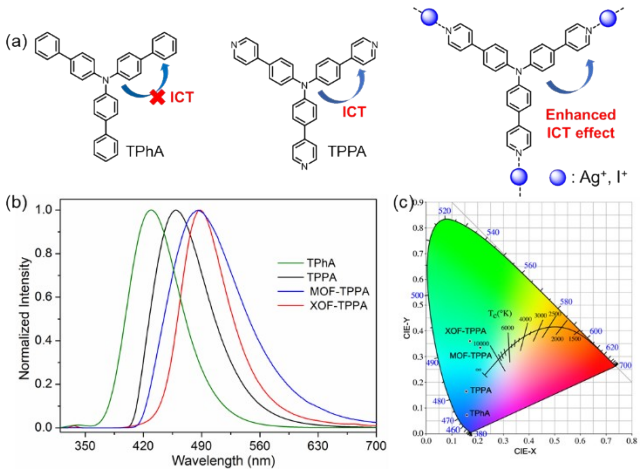

Fig. S20. (a) The ICT effect of **TPhA**, **TPPA** and **MOF/XOF-TPPA**; (b) The normalized fluorescence spectrum of **TPhA**, **TPPA** and **MOF/XOF-TPPA**; (c) 1931 CIE chromaticity coordinates changes of **TPhA**, **TPPA** and **MOF/XOF-TPPA**.

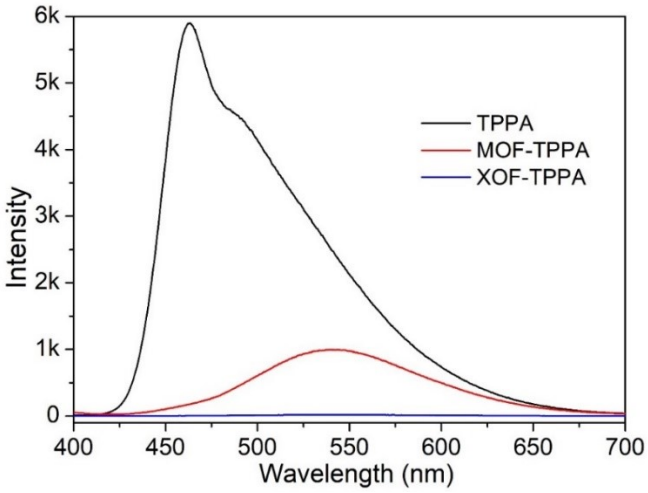

Fig. S21. Fluorescence spectra of the solid power of **TPPA**, **MOF-TPPA** and **XOF-TPPA** (λ_{ex} = 360 nm, Ex/Em slit = 5/1 nm).

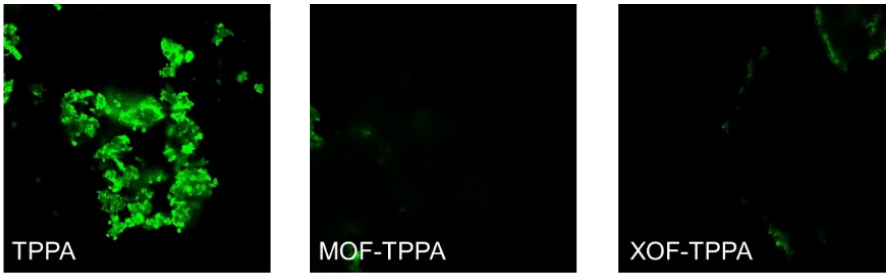

Fig. S22. LSCM images of **TPPA**, **MOF-TPPA** and **XOF-TPPA**

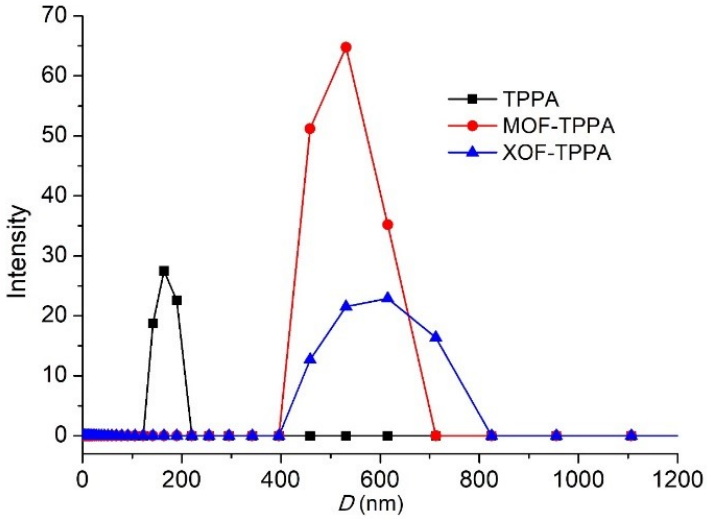

Fig. S23. DLS results of **TPPA**, **MOF-TPPA** and **XOF-TPPA** in **DMSO** (saturated solutions), respectively.

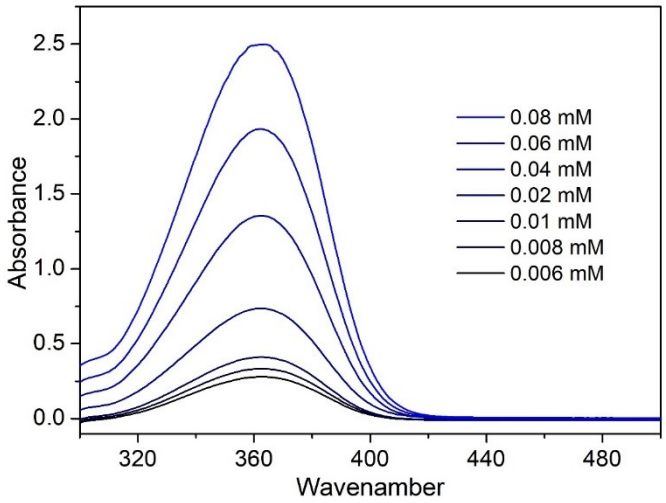

Fig. S24. UV-Vis spectra of **MOF-TPPA** in DMSO.

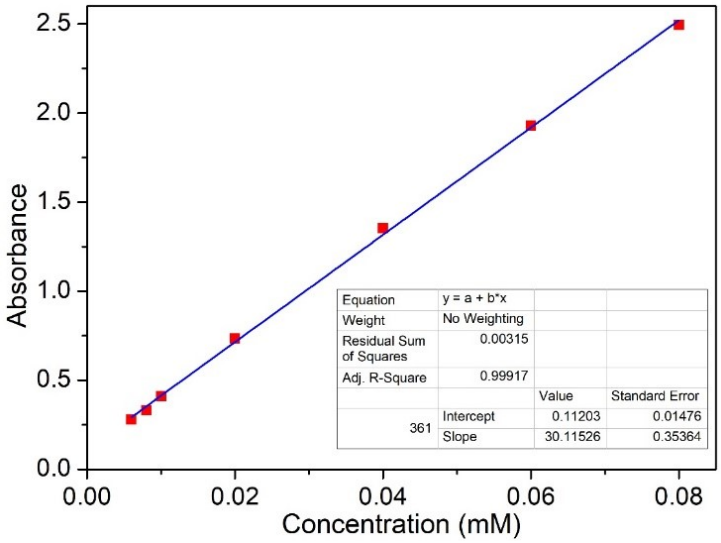

Fig. S25. Plots of concentration vs. absorbance intensity of **MOF-TPPA** at 361 nm in DMSO.

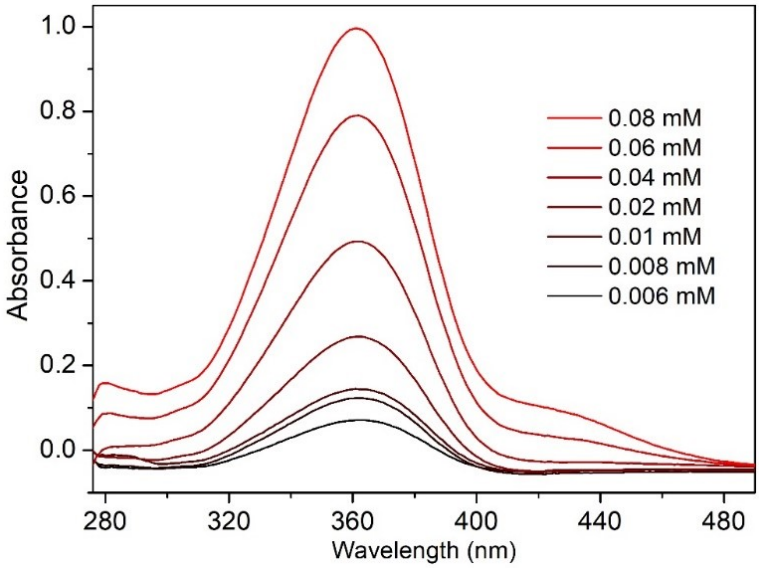

Fig. S26. UV-Vis spectra of **XOF -TPPE** in DMSO.

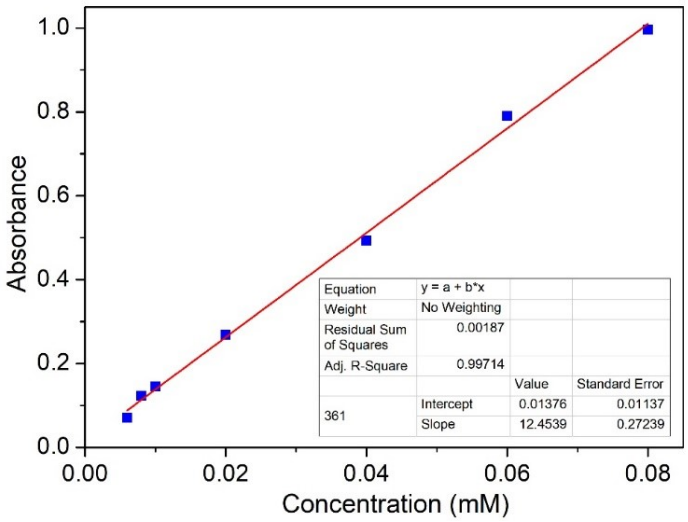

Fig. S27. Plots of concentration vs. absorbance intensity of **XOF-TPPA** at 361 nm in DMSO.

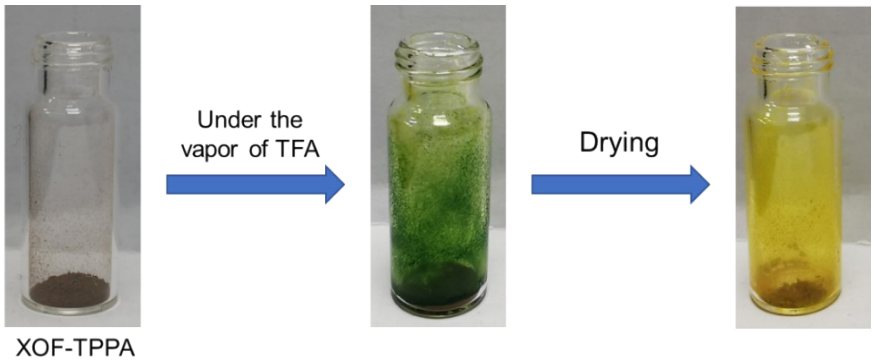

Fig. S28. The picture of XOF-TPPA response to TFA vapor.

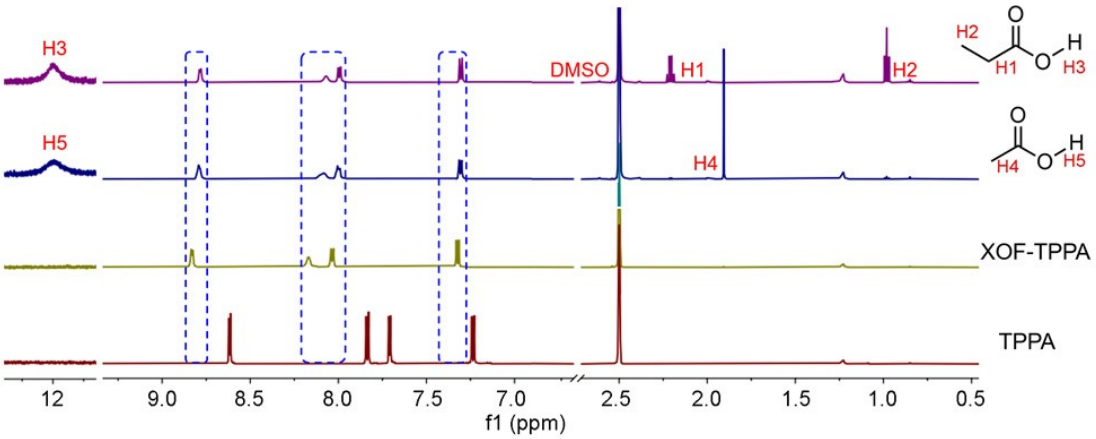

Fig. S29. Partial ^{1}H NMR spectra of **TPPA**, **XOF-TPPA**, and **XOF-TPPA** after treating with MeCOOH and EtCOOH vapors. (DMSO-d_6, 298 K).

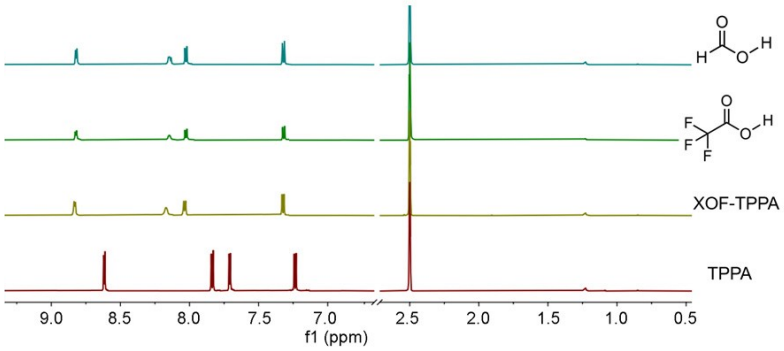

Fig. S30. Partial ^{1}H NMR spectra of **TPPA**, **XOF-TPPA**, and **XOF-TPPA** after treating with TFA and HCOOH vapors. (DMSO-d_6, 298 K).

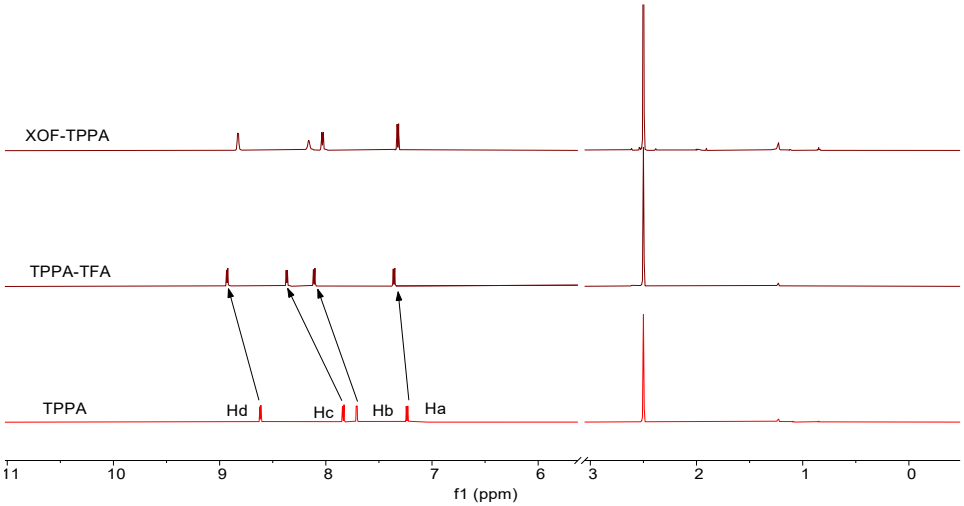

Fig. S31. Partial ^{1}H NMR spectra of **TPPA**, **XOF-TPPA** and **TPPA** after treating with TFA vapor. (DMSO-d_6, 298 K).

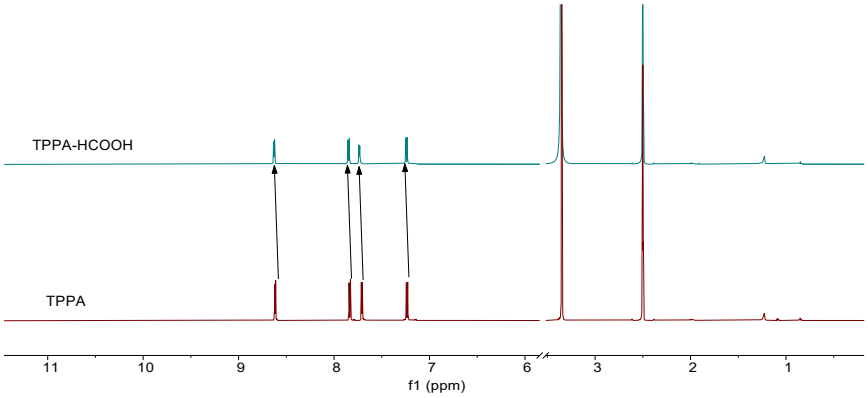

Fig. S32. Partial ^{1}H NMR spectra of **TPPA**, and **TPPA** after treating with HCOOH vapor. (DMSO-d_6, 298 K).

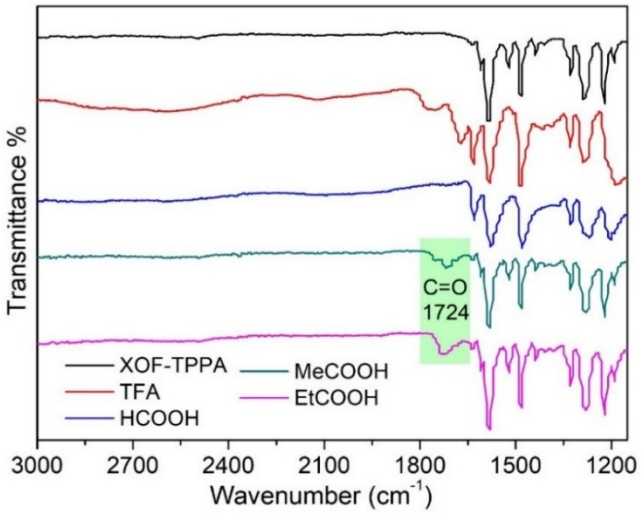

Fig. S33. IR spectra of **XOF-TPPA** and **XOF-TPPA** after exposure to various acid vapors.

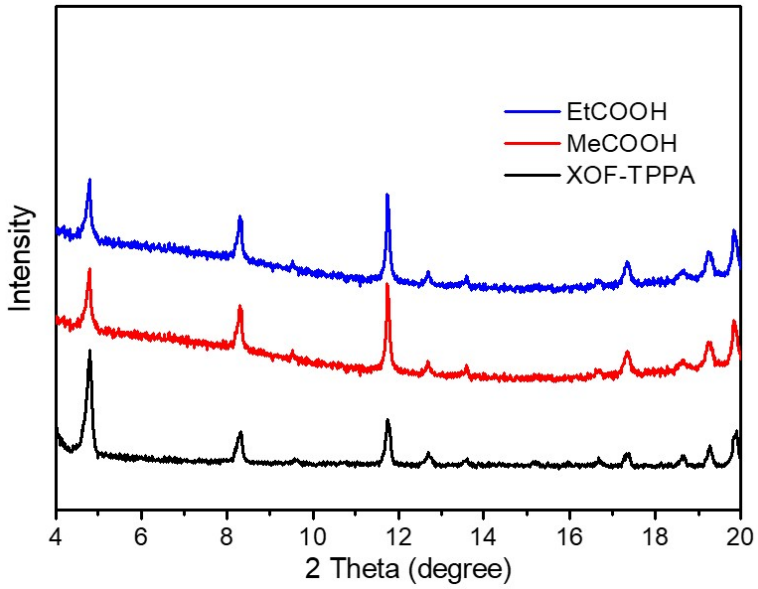

Fig. S34 Experimental PXRD pattern of **XOF-TPPA** and **XOF-TPPA** after three cycles of adsorption.

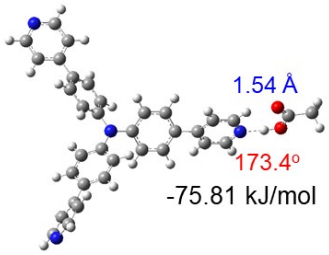

Fig. S35. Optimized geometries of **TPPA**@MeCOOH complex (pyridyl N^1…H-O-R).

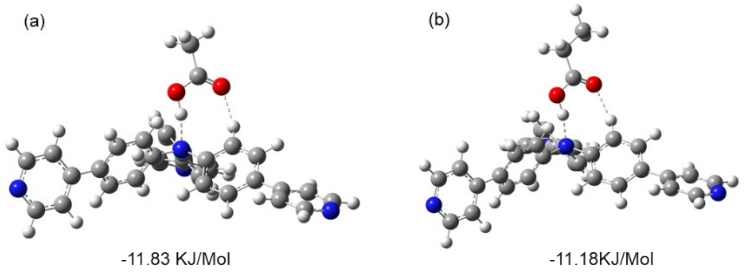

Fig. S36. Optimized geometries of **TPPA** with MeCOOH (a) and EtCOOH (b) complexes (amino N^2…H-O-R).

References

1. Müller, P.; Grünker, R.; Bon, V.; Pfeffermann, M.; Senkovska, I.; Weiss, M. S.; Feng, X.; Kaskel, S., Topological control of 3, 4-connected frameworks based on the Cu2-paddle-wheel node:tboorpto, and why? *CrystEngComm* **2016,** *18* (42), 8164-8171.

2. Zhang, M.-D.; Di, C.-M.; Qin, L.; Yao, X.-Q.; Li, Y.-Z.; Guo, Z.-J.; Zheng, H.-G., Diverse Structures of Metal–Organic Frameworks Based on a New Star-Like Tri(4-pyridylphenyl)amine Ligand. *Cryst. Growth Des.* **2012,** *12* (8), 3957-3963.